Journal of Science and Technology – Engineering and Technology for Sustainable Development
Volume 36, Issue 3, October 2026, 001–009

Green Synthesis of ZnO Materials and Investigation of Methylene Blue Degradation under Ultraviolet Light

Lai Tien Hoa[1], Nguyen Thi Tuyet Mai[2,*], Ta Ngoc Dung[2], Luu Thi Lan Anh[1], Huynh Dang Chinh[2]

[1]*Faculty of Engineering Physics, Hanoi University of Science and Technology, Ha Noi, Vietnam*
[2]*School of Chemistry and Life Sciences, Hanoi University of Science and Technology, Ha Noi, Vietnam*
[*]*Corresponding author email: mai.nguyenthituyet@hust.edu.vn*

Abstract

Toxic dyes represent a critical environmental issue that requires effective treatment due to their direct and indirect impacts on human health. In this experimental study, ZnO nanomaterials were successfully synthesized via a green approach, and several influencing parameters - including stirring temperature, calcination temperature, and calcination time - were systematically investigated, resulting in superior degradation efficiency toward Methylene blue (MB) and the establishment of an optimized synthesis procedure. The phase structure and material properties of ZnO were characterized using X - ray diffraction (XRD), diffuse reflectance spectroscopy (DRS), and UV-Vis light absorption analysis in photocatalytic processes, providing information on particle size, crystalline phase, optical band gap energy, and photocatalytic performance. The results show that the studied parameters significantly affect the characteristics and photocatalytic efficiency of ZnO. Specifically, they show that the ZnO nanomaterials had an average crystal size ranging from 35-40 nm. The ZnO sample at 450 °C showed relatively uniform spherical particles with high porosity, evenly dispersed on the material surface. The band gap energies of the material ranged from 3.19-3.26 eV, which was lower than the Eg of typical ZnO (3.37 eV). The photocatalytic efficiency of MB degradation achieved by the material calcined at high temperatures from 450–700 °C was higher than that of ZnO material calcined at low temperatures. The highest photocatalytic efficiency of MB degradation was achieved by the ZnO sample calcined at 450 °C, reaching 80.85% after 90 minutes under UV-Vis light irradiation, with the highest degradation rate constant of 0.0187 min^{-1}.

Keywords: Green synthesis, Methylene blue, Peristrophe bivalvis extract, ZnO nanomaterials.

1. Introduction

ZnO is one of the most abundant and widely studied oxide semiconductor materials in the Earth's crust, second only to iron oxides [1]. In its mineral form, zincite, ZnO typically exists as a white powder. Historical records dating back thousands of years indicate that as early as 2000 BCE, ZnO was used in ointments to treat various skin diseases in ancient Egypt, and it was later adopted in Roman society. During the Middle Ages, ZnO was employed in brass production in Europe and became widespread in regions of Central and East Asia. By the eighteenth century, ZnO had gained popularity in watercolor art. The introduction of the French process further expanded its application in oil painting [1]. Nowadays, ZnO is one of the most vital materials in diverse fields, especially photocatalysis. This material typically crystallizes in three phases: wurtzite, zinc blende, and rock-salt [2]. Among these, the hexagonal phase is the most stable and dominant among the three phases. At present, various approaches have been developed for ZnO synthesis. Among them, the sol - gel method enables effective control of particle size and operates at relatively low processing temperatures. However, it suffers from prolonged gelation times, the need to remove large volumes of solvent, and a high susceptibility to shrinkage and cracking during the drying process [3]. The heat treatment method is relatively simple but requires relatively high calcination temperatures (around 500 °C) and does not allow for control of crystal particles size. These crystals particles often tend to coagulate into larger crystals particles (~ 60-90 nm) [4]. Chemical vapor deposition (CVD) enables the fabrication of highly oriented and well - crystallized ZnO structures. Nevertheless, it is associated with high cost [5]. The microwave-assisted method offers short synthesis times and uniform energy distribution. Yet, this fabrication method is prone to particle agglomeration and relies on relatively expensive equipment [6]. Escalating textile dye pollution demands efficient photocatalysts for advanced wastewater treatment. This study focuses on the eco-friendly green synthesis of ZnO materials [7]. This is an abundant and cost-effective material with a wide bandgap (~3.37 eV), ZnO enables efficient absorption and photocatalytic degradation under UV radiation. Consequently, green-synthesized ZnO is highly suitable for both research and practical applications [8].

This study utilizes Vietnam's widely available Peristrophe bivalvis extract, leveraging its constituent

p-ISSN 3093-3242
e-ISSN 3093-3579
https://doi.org/10.51316/jst.193.etsd.2026.36.4.x
Received: Dec 31, 2025; Revised: Mar 27, 2026;
Accepted: May 12, 2026; Online: Jun 25, 2026

anthocyanins, flavonoids, and chlorophyll as reducing and stabilizing agents for ZnO synthesis [9, 10]. Furthermore, several parameters affecting the material properties and photocatalytic dye degradation performance were systematically investigated, including the temperature during magnetic stirring with heating, calcination temperature, calcination time, and the precursor ratio between the zinc salt and Peristrophe bivalvis leaf extract. X - ray diffraction (XRD) was employed to determine the possible crystalline phases of the material and to partially estimate the crystallite size and the degree of lattice strain. Subsequently, diffuse reflectance spectroscopy (DRS) was used to determine the optical band gap [11]. Finally, UV-Vis light absorption measurements during the photocatalytic process were conducted to evaluate the degradation efficiency and ensure the reliability of the obtained results.

2. Materials, Experimental Procedure and Methods

2.1. Materials

Materials used included: Peristrophe bivalvis leaf powder purchased from the local market in Vietnam, Zinc nitrate hexahydrate ($Zn(NO_3)_2 \cdot 6H_2O$, 99%, AR-China), Methylene blue (MB) dye ($C_{16}H_{18}ClN_3S$, 95%, Sigma Aldrich), Distilled water.

2.2. Peristrophe Bivalvis Leaves Extraction Procedure

Fig. 1 illustrates the schematic Peristrophe bivalvis extraction process from leaf powder.

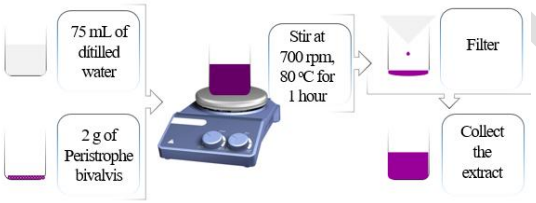

Fig. 1. Schematic diagram of the Peristrophe bivalvis extraction process from leaf powder

A beaker containing 75 mL of distilled water was prepared, to which 2 g of Peristrophe bivalvis powder was added. The mixture was magnetically stirred and heated at 80 °C for 1 h to facilitate the extraction process. After extraction, the resulting solution contained organic compounds derived from Peristrophe bivalvis. The mixture was subsequently filtered using Whatman filter paper to remove solid residues, yielding the Peristrophe bivalvis extract.

2.3. ZnO Nanomaterials Synthesis Process

Fig. 2 illustrates the schematic diagram of the synthesis process of the ZnO sample using $Zn(NO_3)_2$ as the precursor. A solution containing 30 mL of $Zn(NO_3)_2$ was mixed with 30 mL of the previously prepared extract and magnetically stirred while being heated at 70 °C for 1 h. The mixture was then dried at 80 °C for 36 h, yielding a ZnO solid containing organic impurities. The obtained solid was subsequently calcined at 450 °C for 30 min to remove the impurities and obtain ZnO nanoparticles (nanomaterials - NMs). In Table 1, several parameters affecting the photocatalytic efficiency are investigated, including the magnetic stirring temperature, the calcination time, and the calcination temperature. This investigation aims to identify the optimal parameters for the material synthesis process.

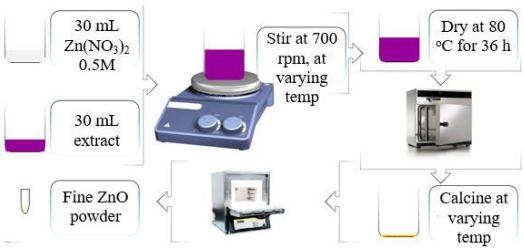

Fig. 2. Schematic illustration of the green synthesis route for ZnO nanomaterials

Table 1. Investigation of parameters affecting the properties of ZnO nanomaterials

Sample	Value	Parameter
H0	-	Non - calcined sample
H5	60 °C	Investigation of heating - stirring temperature
H6	70 °C	
H7	80 °C	
H8	90 °C	
H9	350 °C	Calcination temperature
H10	400 °C	
H6	450 °C	
H11	500 °C	
H12	700 °C	
H13	15 min	Calcination time
H6	30 min	
H14	45 min	
H15	60 min	

2.4. Photocatalytic Experimental Procedure

To evaluate the photocatalytic efficiency of the synthesized samples, the photocatalytic procedure was performed as illustrated in Fig. 3. An amount of 20 mg of ZnO nanomaterial was added to 50 mL of a 5 ppm MB dye solution. The mixture was stirred in the dark for 60 min to reach adsorption-desorption equilibrium, after which a 5 mL aliquot was withdrawn for UV-Vis spectroscopic analysis. Next, the mixture was irradiated under a 250 W OSRAM lamp (emitting in the UVA-UVB region). During irradiation, 5 mL aliquots were collected every 30 min to monitor the degradation progress via UV-Vis spectroscopy.

+ Material Characterization. The crystalline structure and phase purity of the synthesized ZnO nanomaterials were investigated by X-ray diffraction

(XRD) using Cu-Kα radiation (λ = 1.54065 Å) with a scan rate of 0.03°/2s over a 2θ range of 25-80°. Diffuse reflectance spectroscopy (DRS) was performed using a JASCO V-750 solid-state UV-Vis spectrophotometer equipped with a 60 mm integrating sphere at a scan rate of 200 nm/min to determine the optical absorption properties and band gap energy (Eg) of the samples. Additionally, the photocatalytic degradation of the MB dye solution was monitored by measuring the liquid UV-Vis absorption spectra on a HACH DR3900 UV-Vis spectrophotometer.

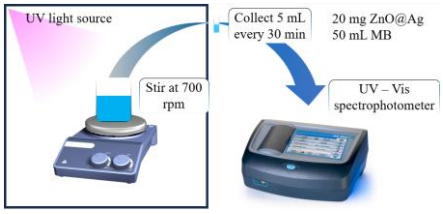

Fig. 3. Photocatalytic process for MB degradation

3. Result and Discussion

3.1. Effect of Magnetic Stirring Temperature on ZnO Nanomaterials Properties

In this investigation, four samples were synthesized with keeping all other parameters constant, but varying the magnetic heating-stirring temperature at 60, 70, 80, and 90 °C, corresponding to samples H5, H6, H7, and H8, respectively.

3.1.1. X-ray diffraction analysis

Fig. 4 was XRD patterns of ZnO NMs samples investigated under varying stirring temperature: H0 (stirring temperature at 70 °C and without calcination), H5 (stirring temperature 60 °C), H6 (stirring temperature 70 °C), H7 (stirring temperature 80 °C), and H8 (stirring temperature 90 °C). The XRD patterns of the ZnO samples (H0, H5-H8) (Fig. 4) confirm that all samples are fully crystallized in the hexagonal wurtzite structure. The major diffraction peaks appear at 2θ approximately 31.8°, 34.4°, 36.3°, 47.5°, 56.6°, 62.8°, 66.3°, 67.9°, and 69.1°, corresponding to the crystal planes (100), (002), (101), (102), (110), (103), (200), (112), and (201), respectively, according to the JCPDS 01-079-0206 standard (JCPDS st.) [12]. The observation of all these peaks, matching well with the standard pattern, indicates that the material phase is pure ZnO, with no significant presence of secondary phases such as other compounds containing Zn^{2+}, metallic Zn, or other oxides - an important conclusion. This is a crucial finding, as secondary phases can distort the absorption bands, complicate the determination of the optical band gap, and alter the photocatalytic mechanism. The sharpness and intensity of the XRD peaks reflect the crystallinity of the material - the sharper and higher the peaks, the better the crystallinity. For the non calcined sample H0, background noise and peaks not belonging to any ZnO phase were observed [13]. This may be due to the presence of residual materials during the ZnO synthesis, which cover the ZnO layer. Calcination helps decompose most of the remaining substance in the material, such as organic compounds, and converts zinc hydroxide into zinc oxide. For samples H5 - H6, the peaks are sharp and intense, reflecting the crystallinity of the material. However, the peak patterns of the samples do not show significant changes, which suggests that the stirring temperature during the ZnO synthesis process does not have a notable effect on the material properties.

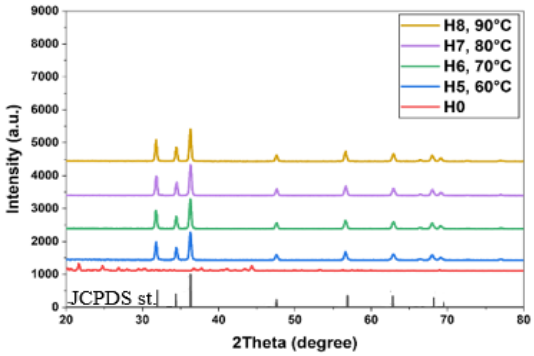

Fig. 4. XRD patterns of ZnO NMs samples

Table 2. Crystal size, strain, and the determination factor of H0, H5-H8 samples determined by the Williamson-Hall method

Sample	Crystal size (nm)	Microstrain (%)	R^2
H0	-	-	-
H5, 60 °C	39.5	1.3	0.9
H6, 70 °C	39.28	1.24	0.95
H7, 80 °C	35.83	1.04	0.94
H8, 90 °C	37.88	1.1	0.92

Through Williamson-Hall analysis (Table 2), the crystallite size, lattice strain, and determination factor of samples H5, H6, H7, and H8 were found to be 39.5 nm, 1.3 %, 0.9; 39.28 nm, 1.24 %, 0.95; 35.83 nm, 1.04 %, 0.94; and 37.88 nm, 1.1 %, and 0.92, respectively. This indicates a low level of strain, and the determination factors of all four samples are above 0.9, suggesting nearly uniform crystal structures. The particle sizes of all four samples are in the nanoscale and do not change significantly, ranging from 35 to 40 nm. Therefore, the ZnO nanomaterial was successfully synthesized.

3.1.2 Diffuse reflectance spectroscopy analysis

The UV-Vis DRS spectra of the samples are shown in Fig. 5. The H5, H6, H7, and H8 samples all exhibit characteristic absorption bands in the UV-Vis region, indicating electron transitions from the valence band to the conduction band. In the wavelength range of 300–370 nm, the reflectance of the samples is low. From 370–450 nm, the reflectance increases sharply and then rises gradually beyond 450 nm. Based on the slope of the

spectra, the differences in reflectance between the samples are not significant. The H7 and H8 samples synthesized at higher stirring - heating temperatures, show reduced crystal defects and improved crystallinity, which partly enhances the crystallinity of the ZnO material. From the DRS results (Fig. 6), the band gap energy (Eg) of the ZnO nanoparticles was calculated by extrapolation using the first-derivative equation derived from the Kubelka–Munk function. The band gap energies of the H5, H6, H7, and H8 samples are 3.23, 3.23, 3.21, and 3.26 eV, respectively. The variation in Eg over the stirring heating temperature range of 60 – 90 °C is negligible, which can be explained by the fact that, for undoped ZnO, factors such as temperature and reaction time do not significantly affect Eg (the Eg of typical ZnO ranges from 3.2 to 3.37 eV).

3.1.3 Photocatalytic efficiency

Fig. 7 shows the MB degradation efficiency for the H5, H6, H7, H8, MB, and H0 samples. Here, the MB sample used only 50 mL of 5 ppm MB to evaluate the photocatalytic efficiency under ultraviolet lamp irradiation. During 45 min of dark stirring, the maximum absorption peak of MB tended to decrease slightly (~10%). This is attributed to partial adsorption of dye molecules onto the ZnO surface, reducing the MB concentration in the solution and thus lowering the maximum absorption peak. After 90 min illumination, the degradation efficiency of the MB sample reached only 17.78%. The H0 sample, using ZnO material after drying, the maximum absorption peak also decreased by about 10% during 45 min of dark stirring. After 90 min of illumination, the degradation efficiency of H0 reached 35.56%, which is still low. This is attributed to residual organic components remaining on the ZnO surface after drying, which hinder MB molecules from contacting the ZnO surface, reducing the number of active sites available.

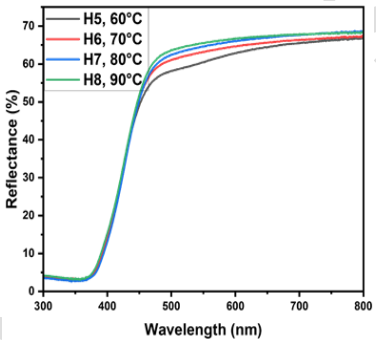

Fig. 5. DRS spectra of ZnO NMs samples (H5-H8)

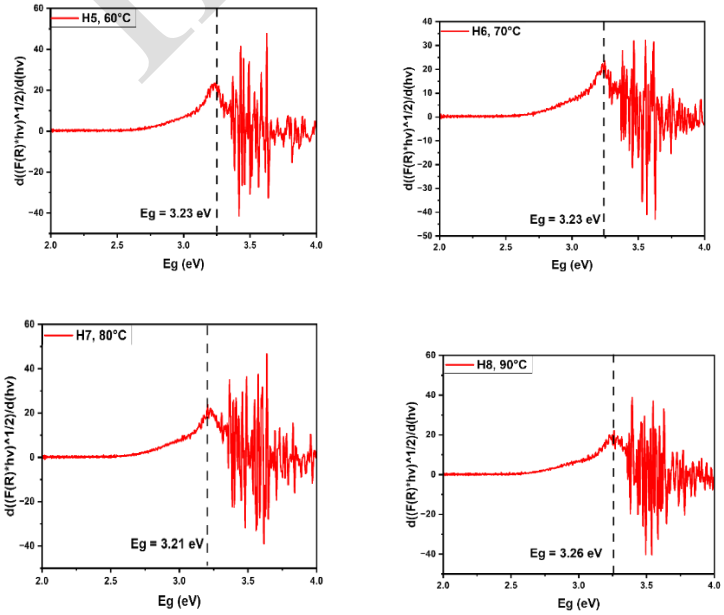

Fig. 6. Derivative results of the DRS analysis for ZnO nanomaterials samples

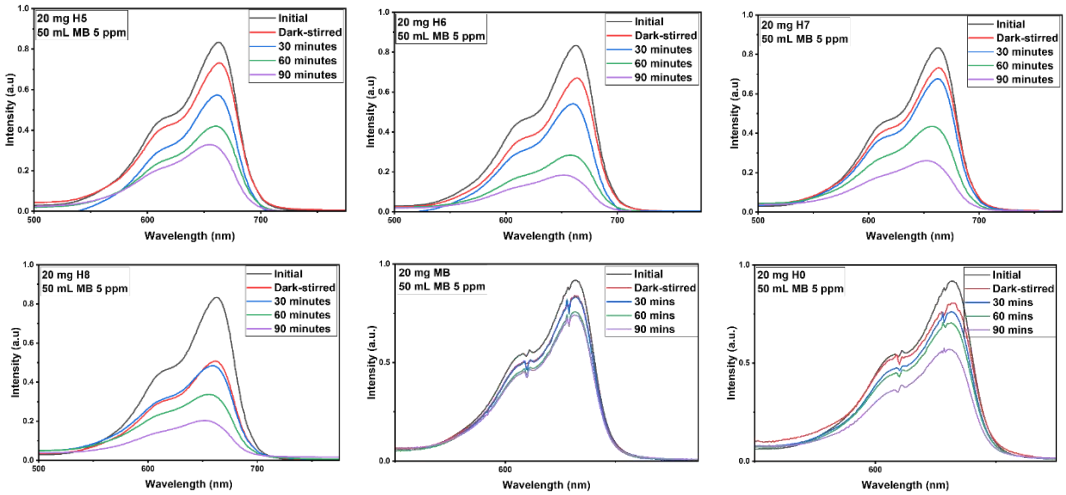

Fig. 7. UV - Vis results of the 5 ppm MB degradation efficiency over time under UV lamp irradiation for samples: H5 (stirring - heating temperature 60 °C), H6 (stirring - heating temperature 70 °C), H7 (stirring - heating temperature 80 °C), H8 (stirring - heating temperature 90 °C), MB (UV irradiation of the MB solution without ZnO catalyst), and H0 (stirring - heating temperature 70 °C without calcination)

Table 3. Reaction rate constants and efficiencies of the H5, H6, H7, H8, MB, and H0 samples

Sample	k (min^{-1})	Efficiency (%)	R^2
H5, 60°C	0.0115	64.89	0.97
H6, 70°C	0.0187	80.85	0.99
H7, 80°C	0.0143	70.34	0.99
H8, 90°C	0.0166	78.72	0.99
MB	0.0023	17.78	0.94
H0	0.0047	35.56	0.97

After calcination, the degradation efficiencies of four samples (H5, H6, H7, and H8) were 64.89, 80.85, 70.34, and 78.72%, respectively. It can be seen that the H6 sample exhibited the highest photocatalytic efficiency, reflecting that the combination of Zn^{2+} and OH^- under these conditions was optimal. The reaction rate constants of the H5, H6, H7, H8, MB, and H0 samples were 0.0115, 0.0187, 0.0143, 0.0166, 0.0023, and 0.0047 min^{-1}, respectively. Clearly showing the correlation that the reaction rate constant is proportional to the photocatalytic efficiency over 90 min of illumination. The determination coefficients of the six samples were all above 0.95 (except MB at 0.94), indicating the reliability of the reported results. Therefore, under the investigation of the effect of temperature during the stirring stage for ZnO synthesis, a temperature of 70 °C resulted in the highest photocatalytic efficiency. Consequently, this condition was selected for subsequent synthesis procedures.

3.2. Effect of Calcination Temperature on ZnO Nanomaterials Properties

This time, for the factor of ZnO calcination temperature, five temperatures were selected such as: 350, 400, 450, 500, and 700 °C, corresponding to the H9, H10, H6, H11, and H12 samples, respectively.

3.2.1 X-ray diffraction analysis

The X-ray diffraction (XRD) patterns of the ZnO sample series (H9-H12, H6) (Fig. 8a) confirm that all samples are fully crystallized in the hexagonal structure. The major diffraction peaks appear at 2θ approximately 31.8°, 34.4°, 36.3°, 47.5°, 56.6°, 62.8°, 66.3°, 67.9°, and 69.1°, corresponding to the crystal planes (100), (002), (101), (102), (110), (103), (200), (112), and (201), respectively (according to the JCPDS 01-079 0206 standard (JCPDS st.)) [12]. The sharpness and intensity of the XRD peaks reflect the crystallinity of the material - the sharper and higher the peaks, the better the crystallinity. Based on the peak intensities of the five samples, it can be seen that the H9 and H10 samples have lower peak intensities than H6, H11, and H12, relatively, the intensities can be ranked as: H9 < H10 < H6 < H11 < H12. This is attributed to the fact that higher calcination temperatures improve the crystallinity of ZnO and reduce the amount of residual organic material, thereby increasing the material's presence.

Fig. 8b shows the Williamson-Hall analysis of the XRD data for the H9, H10, H6, H11, and H12 samples from which the crystallite size and lattice strain were obtained. The values for H9, H10, H6, H11 and H12 samples are 39.5 nm and 1.07 %, 34.07 nm and 0.91 %, 39.28 nm and 1.24 %, 40.42 nm and 1.34 %, 40.07 nm, and 1.45 %, respectively. Thus, the H10 sample has the smallest particle size, while the H11 sample has the largest. The lattice strain of the five samples are relatively

low. Therefore, the green synthesis successfully produced nanosized particles, achieving the intended increase in surface area.

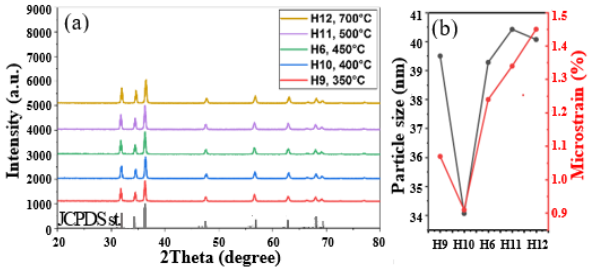

Fig. 8. XRD patterns: (a)- plots showing crystallite size and lattice strain, (b)- ZnO samples investigated with respect to calcination temperature (H9 (350 °C), H10 (400 °C), H6 (450 °C), H11 (500 °C), and H12 (700 °C))

3.2.2. Diffuse reflectance spectroscopy analysis

To check the reflectance and band gap energy of the samples, we conducted DRS measurements and analyzed the results for the five samples: H9, H10, H6, H11, and H12. From Fig. 9a, the H9, H10, H6, H11, and H12 samples all exhibit characteristic absorption bands in the UV-Vis region, indicating electron transitions from the valence band to the conduction band. In the wavelength range of 300-370 nm, the reflectance of all samples is low. From 370-450 nm, the reflectance increases sharply and then rises gradually beyond 450 nm. The H9 and H10 samples have higher reflectance than H6 and H11 samples from 450 nm onward, which may indicate that H6 and H11 have more defects (Fig. 9b), leading to reduced reflectance. For the H12 sample, the high calcination temperature (700 °C) enhances the crystallinity. Fig. 9b shows the band gap energies of the five samples. At a calcination temperature of 350 °C, Eg is 3.19 eV, and when the temperature increases to 400 °C, Eg is 3.2 eV. From 450-700 °C, the Eg of ZnO remains at 3.23 eV. This indicates that as the calcination temperature increases, the band gap of the material gradually widens but not significantly, suggesting that increasing the calcination temperature from 350-700 °C helps improve crystallinity and reduces lattice deviations.

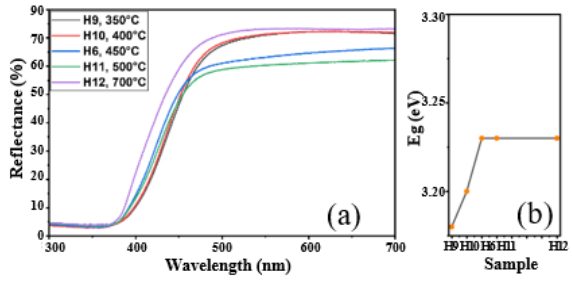

Fig. 9. (a)- DRS results of ZnO samples investigated for the effect of calcination temperature of of H9, H10, H6, H11 and H12 samples; (b)- Eg of these samples

3.2.3. Photocatalytic efficiency

The first-order kinetic plots over time (Fig. 10) for H9, H10, and H11 samples show reaction rate constants of 0.0082, 0.0081, and 0.0132 min^{-1}, respectively. This is indicating slower increases compared to H6 and H12 samples (0.0187 min^{-1} and 0.0162 min^{-1}, respectively). This reflects that at calcination temperatures of 350 °C and 400 °C, the photocatalytic efficiency of the material is not high (53.19% and 55.32%, respectively). Therefore, it is suggested that the calcination temperature is not sufficient to remove organic components in the materials, leading to surface coverage of ZnO and reduced efficiency. For H6 sample, the efficiency reaches the highest value of 80.85%, indicating that organic impurities were sufficiently removed while still acting as stabilizers to optimize particle size, increase surface area, and enhance reaction efficiency. For H11 and H12 samples, the efficiencies are 73.4% and 75.53%, respectively. This is showing that at higher temperatures (500–700 °C), organic components decompose, reducing their stabilizing role, but the high-temperature calcination improves crystallinity, which contributes to the overall material efficiency. Table 4 shows the kinetic equations corresponding to Fig. 11. In addition, the determination coefficients of H9, H10, and H11 samples are not high (0.86, 0.8, and 0.83, respectively), indicating that the equations do not fully reflect the experimental results. The H6 and H12 show high reliability (0.98 and 0.96), suggesting that the assumed kinetic model is consistent with the actual results.

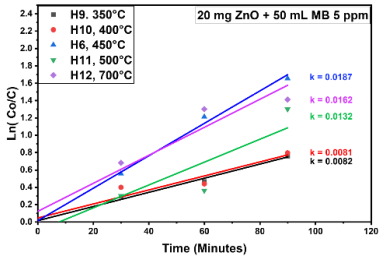

Fig. 10. First - order kinetic curves of H9, H10, H6, H11, and H12 samples

Therefore, under the investigation of calcination temperatures from 350–700 °C, the sample calcined at 450 °C (H6) showed the highest degradation efficiency compared to the other samples. Thus, a calcination temperature of 450 °C will be selected for subsequent experiments. Based on XRD, DRS analyses of the two conditions, calcination temperature and stirring heating temperature, it can be confirmed that the materials all exhibit hexagonal ZnO phase structure and band gap energies ranging from 3.19–3.26 eV (consistent with ZnO). Therefore, in the following results the photocatalytic process will only be studied under these conditions to determine optimal efficiency.

Table 4. First - order kinetics, degradation efficiency, and determination coefficients of of H9, H10, H6, H11, and H12 samples

Sample	Reaction kinetic equation	Efficiency (%)	R^2
H9	$Ln(C_0/C)=0.0423+ 0.0077*t$	53.19	0.96
H10	$Ln(C_0/C)=0.146+ 0.0066*t$	55.32	0.83
H6	$Ln(C_0/C)=0.0408+ 0.0183*t$	80.85	0.98
H11	$Ln(C_0/C)=-0.3629+ 0.0171*t$	73.4	0.80
H12	$Ln(C_0/C)=0.4215+ 0.0121*t$	75.53	0.86

3.3. Effect of Calcination Time on Photocatalytic Efficiency of ZnO NMs

For the factor of calcination time, the durations of 15, 30, 45, and 60 min were investigated, corresponding to the H13, H6, H14, and H15 samples, respectively. Table 5 shows the first-order kinetic equations, determination coefficients, and photocatalytic efficiencies of four samples (H13, H6, H14, and H15). Based on the determination coefficients, the assumed kinetic models of the four samples are relatively reliable and consistent with the experimental results. The reaction rate constants of the H15, H14, H6, and H13 samples are 0.006 min^{-1}, 0.012 min^{-1}, 0.0187 min^{-1}, and 0.0127 min^{-1}, respectively. These are indicating that H13, H14, and H15 have much lower degradation rates compared to H6. It suggests that at a calcination temperature of 450 °C, the residence time for H13 was insufficient to fully decompose the organic components, resulting in low degradation efficiency (68.89%). When the sample was held for 30 min, H6 showed significantly higher efficiency compared to H14 and H15 (66.67% and 44.44%, respectively). This indicates that 30 min of calcination is sufficient to improve crystallinity while maintaining large surface area and effective active sites better than holding the sample for 1 hour. Although crystallinity improves, the reduction of organic components leads to particle aggregation, which decreases surface area and reduces active sites. Therefore, under the investigation of sample residence times from 15 min to 1 hour at 450 °C, the H6 sample showed better MB degradation performance compared to the three other samples. Thus, under this condition, a calcination time of 30 min will be selected for the next investigation. Therefore, under the investigation of sample residence times from 15 min to 1 hour at 450 °C, the H6 sample showed better MB degradation performance compared to the three other samples. Therefore, under these conditions, a calcination time of 30 minutes for the ZnO nanomaterials (NMs) sample should be selected for further research to achieve the optimal photocatalytic effect in the ultraviolet irradiation region.

Table 5. MB degradation efficiency of ZnO NMs

20 mg catalyst + 50 mL MB 5 ppm			
Sample	Reaction kinetic equation	R^2	Efficiency (%)
H13	$y= 0.0127x + 0.0519$	0.99	68.89
H6	$y= 0.0187x + 0.0123$	0.99	80.85
H14	$y= 0.012x + 0.0487$	0.98	66.67
H15	$y= 0.006x + 0.0657$	0.90	44.44

3.4. Scanning Electron Microscopy of ZnO NMs

Fig. 11 shows scanning electron microscopy at 10 µm and 20 µm dimensions of H9 and H6 samples fabricated by the green method using Peristrophe bivalvis extract solution. Based on the SEM images in Fig. 11, the surface morphological characteristics of the samples are shown. The H9 sample shows particles adhering together, lacking porosity and with unclear particle shapes. Meanwhile, the H6 sample shows relatively uniform spherical particles with high porosity, evenly dispersed over the material surface. These SEM results partly explained and demonstrated the results regarding the photocatalytic efficiency of MB degradation of H9 samples (53.19%) and H6 (80.85%) samples as shown in Table 4.

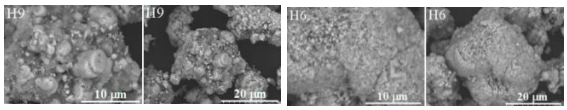

Fig. 11. Scanning electron microscopy at 10 µm and 20 µm dimensions of H9 and H6 samples

3.5. Results Comparing Photocatalytic Performance with ZnO Samples from Other Studies

Table 6 shows the comparative results of the photocatalytic degradation performance of MB dyes by ZnO NMs in this study with results from other studies. From the results of comparison Table 6, it can be observed that the ZnO NMs samples fabricated using the green method in our study also achieved relatively good performance. Of course, the direction is to improve the conditions to achieve higher efficiency for this material, (given that this research was conducted in a still rudimentary laboratory with limited investment, and this research is mainly to support students in their graduation projects and subsequent postgraduate studies).

Table 6. Comparative results of the photocatalytic performance of MB dyes with results from other studies

Sample [Ref.]	ZnO NMs (H6) [This study]	ZnO NPs (Z1) [[Ref.15]	ZnO NPs [[Ref.16]
Fabri--cated method	Green method using Peristrophe bivalvis extract	39.28 nm, 3.23 eV, uniform spherical particles with high porosity	80.58% 5ppm MB solution in 90 mins under illumination of Osram 250W lamp.
Crystal size, Eg, surface morpho--logy	Green method using plant extracts from Azadir achta indica	25.66 nm, 3.36 eV, No data of surface morphology	90.25 % of 5 ppm MB in 55 mins under sunlight illumination.
MB Decomp-osition efficiency	Green method using Justicia adhatoda leaf extract	18.57 nm, 3.04 eV, flower-like morphology	99.12% of 10 ppm MB in 120 mins under solar light irradiation.

4. Conclusion

ZnO nanomaterials was successfully synthesized via green method, as clearly confirmed by XRD results showing the hexagonal phase. The results indicate that the particle size is approximately 30 to 40 nm according to Williamson - Hall calculations, exhibiting high crystallinity. DRS results also show that the band gap energy of the material is consistent with previously reported Eg values of ZnO [17]. Factors such as stirring-heating temperature, calcination temperature, and calcination time have significant effects on the structure and the degradation efficiency of MB dye solution. After the investigation, the highest degradation efficiency of 5 ppm MB using ZnO was 80.85% with H6 sample under 90 min of UV light irradiation. Throughout this study, it can be concluded that the green synthesis method of ZnO is suitable for research aiming at low toxicity, environmental friendliness, reasonable cost, and a simple synthesis procedure, providing ZnO nanomaterials with excellent potential for toxic dyes degradation.

Acknowledgments

The authors thank the C1-401 Photocatalytic, Adsorption, and Green Energy Materials Laboratory. The authors thank the C9-110 Optics and Optoelectronics Laboratory. The authors express their sincere gratitude for the valuable technical support and the provision of facilities by the Ceramic Materials Research and Development Laboratory.

References

[1] S. Raha and M. Ahmaruzzaman, ZnO nanostructured materials and their potential applications: Progress, challenges and perspectives, Nanoscale Advances, vol. 4, no. 8, pp. 1868–1925, Apr. 2022. https://doi.org/10.1039/D1NA00828A

[2] C. Zhu and X. Wang, Nanomaterial ZnO synthesis and its Photocatalytic applications: A review, Nanomaterials, vol. 15, no. 9, May 2025, Art. no. 682. https://doi.org/10.3390/nano15090682

[3] B. Eren, M. K. Gunduz, D. Berikten, and Z. B. Bahsi, Therapeutic potential of sol-Gel ZnO nanocrystals: Anticancer, antioxidant, and antimicrobial tri-action, ACS Omega, vol. 9, no. 13, pp. 14818–14829, Apr. 2024. https://doi.org/10.1021/acsomega.3c07191

[4] G. G. di Confiengo, M. G. Faga, Microwave approach and thermal decomposition: A sustainable way to produce ZnO nanoparticles with different chemo-physical properties, Chem. and Phys., 321, 129485, 2024. https://doi.org/10.3762/bjnano.15.112

[5] T.-L. Phan, L. V. Cuong, V. D. Lam, and N. T. Dang, Various CVD-grown ZnO nanostructures for nanodevices and interdisciplinary applications, Beilstein Journal of Nanotechnology, vol. 15, pp. 1390–1399, Oct. 2024. https://doi.org/10.3762/bjnano.15.112

[6] I. Bilecka, P. Elser, M. Niederberger, Kinetic and thermodynamic aspects in the microwave-assisted synthesis of ZnO nanoparticles in benzyl alcohol, ACS Nano, vol. 3, no. 2, pp. 467–477, Feb. 2009. https://doi.org/10.1021/nn800842b

[7] R. Al-Tohamy, S. S. Ali, F. Li, K. M. Okasha, Y. A. Mahmoud, A. A. Elsamahy, H. K. Jiao, Y.-G. Fu, and J. Sun, A critical review on the treatment of dye-containing wastewater: Ecotoxicological and health concerns of textile dyes and possible remediation approaches, J. Hazardous Materials, vol. 387, Mar. 2020, Art. no. 121954. https://doi.org/10.1016/j.jhazmat.2019.121954

[8] C. Zhu and X. Wang, Nanomaterial ZnO Synthesis and its photocatalytic applications: A review. Nanomaterials, vol. 15, no. 9, 682, 2025. https://doi.org/10.3390/nano15090682

[9] P. H. Le, D. N. Dao, T. Q. Huynh, T. T. T. Tran, and V. Nguyen, Extraction and purification of anthocyanins from Peristrophe bivalvis (L.) Merr. using an aqueous two-phase system, J. Food Biochemistry, vol. 45, no. 10, Oct. 2021, Art. no. e13910. https://doi.org/10.1111/jfbc.13910

[10] L. M. Cuong, L. C. Chung, T. T. Thai, and L. T. L. Anh, Investigationof the Cam leaf extraction process oriented to synthesize silver nanoparticles (Ag NPs), Vietnam Journal of Catalysis and Adsorption, vol. 12, no. 1, pp. 85–90, Mar. 2023. https://doi.org/10.51316/jca.2023.014

[11] A. E. Athare, Synthesis and characterisation of ZnO nanoparticals by XRD, EDX, SEM, FTIR and UV-DRS, International Journal of Scientific Research in Science, Engineering and Technology, vol. 4, no. 1, pp. 627–631, 2018.

[12] I. I. C. f. D. Data, PDF Card No. 01-079-0206. Powder Diffraction File, Newtown Square, PA, USA, n.d.

[13] A. Jain, S. P. Ong, G. Hautier, W. Chen, W. D. Richards, S. Dacek, S. Cholia, D. Gunter, D. Skinner, G. Ceder, and K. A. Persson, Commentary: The materials project: A materials genome approach to accelerating materials innovation, APL Materials, vol. 1, no. 1, Jul. 2013, Art. no. 011002. https://doi.org/10.1063/1.4812323

[14] S. Landi, I. R. Segundo, E. Freitas, M. Vasilevskiy, J. Carneiro, and C. J. Tavares, Use and misuse of the Kubelka Munk function to obtain the band gap energy from diffuse reflectance measurements, Solid State Communications, vol. 341, 2022, Art. no. 14573. https://doi.org/10.1016/j.ssc.2021.114573

[15] U. U. Pradhan, A. Karanam, M. Raghavan, and R. Krishna, Green synthesis of ZnO nanoparticles using Azadirachxta indica, Coffea arabica, Citrus sinensis and Mimosa pudica extracts: Characterization and photocatalytic degradation of methylene blue dye, Materials Letters, vol. 397, Art. no. 138805(1-9), Sep. 2025. https://doi.org/10.1016/j.matlet.2025.138805

[16] A. B. Anik, M. H. Akash, and M. A. Alam, Greensynthesis of ZnO nanoparticles using Justicia adhatoda for effective photoncatalytic degradation of methylene blue dye, RSC Advances, vol. 15, pp. 45874–45888, Nov. 2025. https://doi.org/10.1039/D5RA06656E

[17] V. Pawar, P. K. Jha, Band-gap engineering in ZnO thin films: A combined experimental and theoretical study, Applied Surface Science, vol. 447, pp. 244–250, Aug. 2018. https://doi.org/10.1016/j.apsusc.2018.04.006